



The phenomenon of magnetic vortices superconducting for (Sr₂RuO₄)

Hussein Ali Mohammed

Department of Physics , Education Faculty for pure science , University of Kirkuk , Kirkuk , Iraq

DOI: <http://dx.doi.org/10.25130/tjps.23.2018.134>

ARTICLE INFO.

Article history:

-Received: 18 / 3 / 2018

-Accepted: 3 / 5 / 2018

-Available online: / / 2018

Keywords: Sr₂RuO₄ single crystals samples, 2DEG Hall-probe sensor ,scanning Hall probe microscopy technique.

Corresponding Author:

Name: Hussein Ali Mohammed

E-mail:

hussein_ali722002@yahoo.com

Tel:

1.Introduction

Strontium Ruthenate was first synthesised in 1959 [1]. It has a tetragonal layered perovskite structure in common with the high-T_c cuprates as shown in Fig. 1.; however unlike the cuprates, Sr₂RuO₄ is a conductor at room temperature in the absence of chemical doping. Scientific focus fell on Sr₂RuO₄ because of its structural similarities with the cuprates but it wasn't found to be superconducting until 1994 [2], eight years after the discovery of superconductivity in the cuprates. One reason for this

Abstract

The study of superconducting vortices have been describes by a series of magnetometry experiments conducted on unconventional superconductors which is Sr₂RuO₄, using Scanning Hall probe microscopy technique (SHPM) (T_c ≈ 1.5 K). In this study have numerous samples as well propose that the vortex behaviour is modified with little amounts of disorder. Experimentally the better chips show a clear field driven triangular to square vortex lattice transition at low fields, as predicted by extended London theory calculations. In stark disparity, somewhat less well-ordered chips exhibit pronounced vortex chaining banding that which tentatively attribute to an extrinsic source of disorder.

delay was that it has a T_c of ~1.5K, two orders of magnitude lower than the cuprates where T_c can be up to ~160K. It was the first layered perovskite superconductor without copper to be discovered. The Ginsburg-Landau coherence length and London penetration depth are estimated to be ξ(0)≈60nm and λ(0)≈150nm making Sr₂RuO₄ a Type II SC with κ≈2.5.

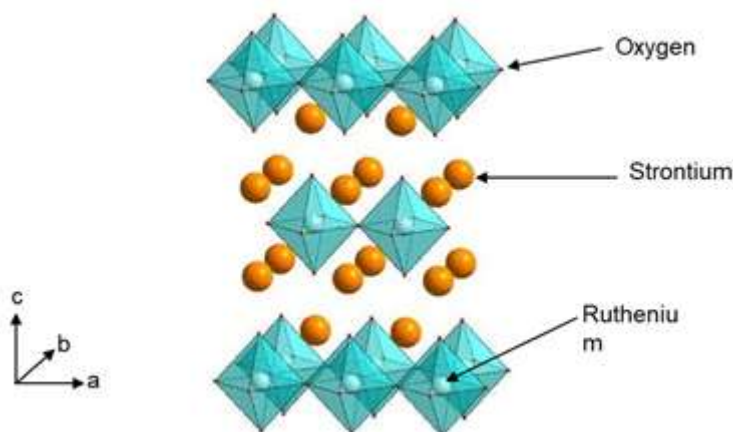


Fig. 1. Schematic of the tetragonal layered perovskite structure of Sr₂RuO₄ [2] .

Sr_2RuO_4 has been the subject of great scientific interest for the past decade and a half; however after numerous experiments the exact nature of the SC is still open to interpretation. After much suspicion the first clear evidence that the superconductivity wasn't s-wave came from the observation that the introduction of non-magnetic impurities affected a significant suppression of T_C [3]. Hasselbach shows that s-wave superconductivity is invulnerable to elastic impurity scattering and so this constitutes a highly valid result. Early bulk magnetic and transport measurements revealed results that bore remarkable similarity to those of superfluid ^3He ; which was known to invoke p-wave spin-triplet atomic bound states [4]. This provided the early motivation to suggest that the superconductivity was spin-triplet based. Subsequent measurements of the Knight shift provided strong evidence in support of this; and further evidence gathered from muon spin rotation (mSR) measurements also point towards p-wave pairing. However, a search for the same evidence as that cited by the μSR by Scanning Hall Probe Microscopy (SHPM) failed to corroborate this success [5].

In parallel with this work, recent theory [6] suggests that a square vortex lattice is anticipated for a p-wave spin-triplet SC and Small Angle Neutron (SAN) measurements appear to confirm this [7]. Continuing with this now familiar pattern of confirmations and contradictions, recent angle dependant specific heat measurements would appear to contest this view of exact nature of the pairing wave function. In

particular, several novel vortex structures are predicted for specific pairing symmetries and the identification and characterisation of these would provide telling insights into the nature of the superconducting order parameter.

2. Experimental

Wafers of the $\text{GaAs}/\text{Al}_{0.3}\text{Ga}_{0.7}\text{As}$ heterostructure are grown using Molecular Beam Epitaxy and are readily available commercially. Patterning into sub-micron hall crosses using conventional Electron Beam Lithography is then a fairly straightforward technique which has been optimised at the University of Bath. The small active area of the hall cross gives excellent spatial resolution to go with high field sensitivity. During the fabrication process all patterning and cleaning steps were performed in the same way as for the ohmic contacts except the resist spin speed was increased to 5000 for 30 seconds. The tip was formed from a 10 nm thick layer of Ti followed by 50 nm layer of Au, as well as the design for making the STM tip places it at the highest point near the corner of the Hall probe to ensure that it comes into contact with the sample first. For that reason a gold tunnelling tip (STM) is incorporated onto the HP substrate in close proximity to the active area using optical lithography which used Scanning Hall Probe Microscopy (SHPM) technique at Bath University. The rate of Helium gas (He) cools the sample from (4.2 to ~ 1.6) K. This is used to detect sample sensor separation. A schematic of the microscope head are shown in Fig. 2.

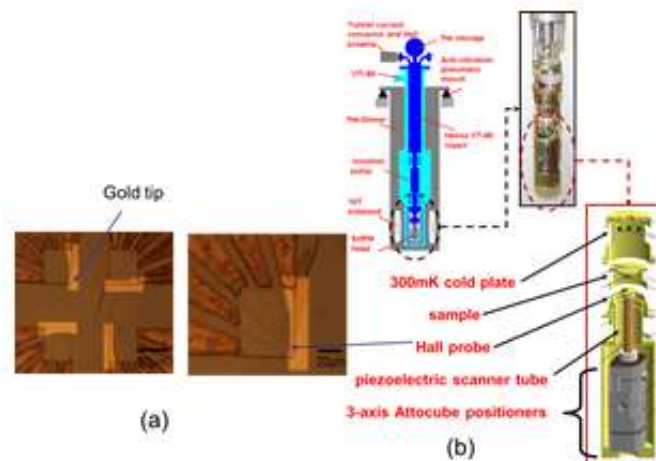


Fig. 2. (a) Optical images of a chip after fine etching at different magnifications and (b) Third Generation Scanning Hall Probe Microscope System (SHPM).

The HP is mounted onto a piezoelectric scanner tube which itself is mounted on 3 coarse scale nanopositioners. The piezo provides a scanning image size of $\sim (14 \times 14) \mu\text{m}$ ($\pm 100\text{V}$) at 300mK. The sample is mounted onto an easily detachable sample holder cup with silver paint and orientated to face the HP. Sample/sensor tilt angle is adjusted by three screws to give $\sim 1^\circ$ offset before approach is attempted [8].

The microscope head is screwed directly into a commercial Variable Temperature Insert (VTI). The cryostat consists of two dewars, the outer being filled with liquid Nitrogen, the inner liquid Helium. The space surrounding the VTI is pumped, and a flow of cold He gas is controlled using a needle valve between the inner dewar and the space surrounding the VTI. A high flow rate of He gas cools the sample from 4.2K to $\sim 1.6\text{K}$.

3.Results and discussion

Measurements have been made on 3 different ultra-pure samples of Sr_2RuO_4 over five separate experiments utilising the apparatus described in above section. Four of the experiments produced useful data; the third in the sequence failed after measurements were compromised by damage to the HP sustained after a contact with the sample. Each crystal was grown by a floating zone method [9] at the University of St Andrews. Initial results look extremely promising, but at face value seem to throw up more questions rather than provide any answers. Unexpected and strange behaviour has been observed in all three samples. All external fields have been applied perpendicular to the crystal surface being scanned. As a result two “signs” of superconducting vortex are shown in the images below (white and black), corresponding to positive and negative coil currents. Due to the current uncertainty in theories of superconductivity in Sr_2RuO_4 and the range of behaviour we have observed, no attempt has yet been made to explain the observations, or indeed present

the observations as evidence of one type of pairing over another. The first experiment didn't produce any radical data but served to validate our overall SHPM approach and provide our first glimpse of superconducting vortices in Sr_2RuO_4 . At 300mk with zero applied field (cooled in earth's field) a generally disordered vortex pattern was observed. Fig.3 shows three images taken at the same temperature, same applied field but different (neighbouring) locations. The density of vortices is seen to vary slightly with location (17, 12, 12 vortices per image). Repeated cycles of heating and cooling through T_c (Fig. 4) revealed that some vortices occupy more or less the same sites each time, while others have moved around. The existence of vortices in the same locations is indication of strong pinning by underlying crystalline disorder. Increasing temperature towards T_c sees the vortices arrange in an Abrikosov-type lattice and revealed what looks like a small forbidden region from which vortices seemed to be expelled. [10]. (Fig. 5). The image size of fig.s 3, 4, and 5 are $\sim 20 \times 20 \mu\text{m}^2$.



Fig .3. Scanning Hall Probe images of Sr_2RuO_4 at three different locations. The sample was cooled in the earth's field. [$T=300\text{mk}$, $H_{\text{APP}}=0$]

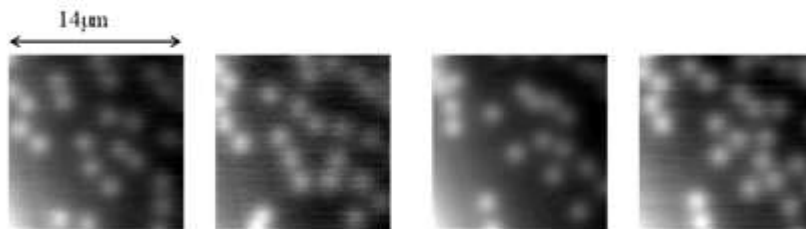


Fig .4. SHPM images of Sr_2RuO_4 . They are taken at the same location at $T=300\text{mk}$ after cycling above and below T_c .

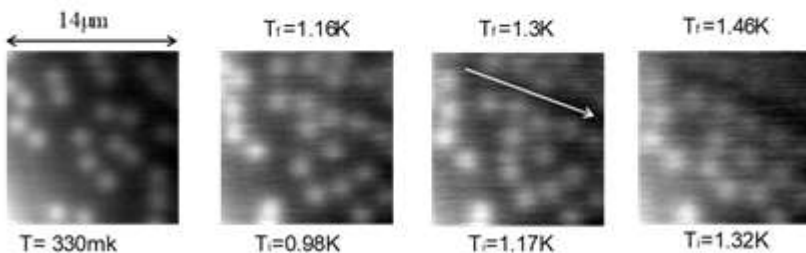


Fig .5. A sequence of images showing vortex behaviour with increasing temperature.

A second sample which is from a different growth batch to the first and has undergone an annealing process was received from Andrews College. Cooling in the earth's field revealed a similar density of vortices as had been observed as sample one. In the location displayed in fig. 6(a) it looks like there could

be another forbidden domain; this time in the vertical direction. Resolution is worse here because unstable tunnel contact was experienced and so the image is taken further from the surface than for the previous images. After cancelling the earth's field by fine tuning the applied field until no vortices were in

view, a striped magnetic structure was exposed. The motion of piezo scanner tube is usually divided into two parts; the lateral raster scan in the XY plane and the topography tracking response in the Z direction. The resulting scanner range is typically between (1-100) μm in XY and (0.1-10) μm in the Z direction. After examining different locations, the period of the fine structure seemed constant ($\sim 1.75\mu\text{m}$) in the Z direction but the pattern varies slightly. (Fig. 6(b) and (c)) but was predominantly vertical in our image axis. Interestingly it remains intact above T_c (d) – it's not superconducting [11].

Increasing the density of vortices by applying ± 10 Oe (white/black vortices) added weight to the existence of vertically aligned 'forbidden' regions as shown in Fig.7. However this was the only other location where this was seen. The underlying fine structure seemed to be aligned with this zone. The period of the fine structure ($\sim 1.75\mu\text{m}$) was found to be temperature (Fig. 8) and field independent (Fig. 9). However, as the line scans displayed in 9(c) show, the contrast appears to have reversed after increasing the temperature to 4.5K. This would be a very interesting result but care needs to be taken, for instance the shift of $\sim 1.75\mu\text{m}$ may have occurred due to thermal expansion; more evidence of this is needed [12].

After discovering the magnetic fine structure, the natural question of how vortices interact with it arose. Fig. 10 illustrates an attempt to establish the pinning centres of some vortices. Dirt particles and surface roughness can sometimes make getting the HP close to the surface problematic but Fig. 10(a) (i) shows an instance when we were fortunate to find a very flat and clean region. As such we were able to image the fine structure and vortices in the same image. Previously contrast was dominated by the vortices and the stripes remained hidden until the remnant (Earths) field was cancelled. A first glance at 10(a)(i) provides good evidence that white vortices were pinned on black stripes and this is confirmed (at this location) by considering the vortex maxima (a)(ii). However, on switching the field and investigating different locations, it became clear that the picture wasn't so simple. At a different location 10(b) shows the stripes (i), vortices (ii) and overlay of the two (iii). In this instance we observe vortices residing on both types of stripe. Unfortunately verifying the nature of any interaction is complicated by the presence of sample inhomogeneity: dislocations, impurities etc. Separating pinning resulting from purely magnetic as to that caused by crystalline disorder is extremely difficult [13].

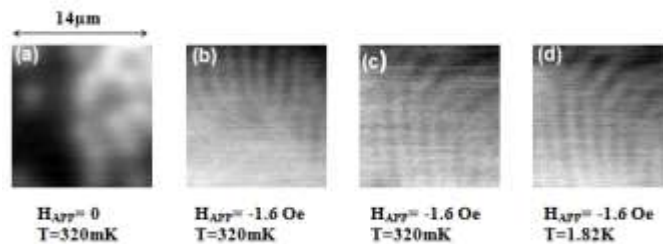


Fig. 6. Various SHPM images taken of sample two. The image size is $\sim 20 \times 20 \mu\text{m}^2$.

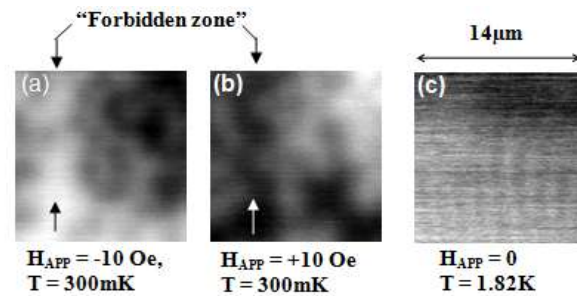


Fig. 7. Shows evidence of both negative (a) and positive (b) vortices being driven out of a linear region that is aligned with the underlying magnetic fine structure (c). The image size is $\sim 20 \times 20 \mu\text{m}^2$.

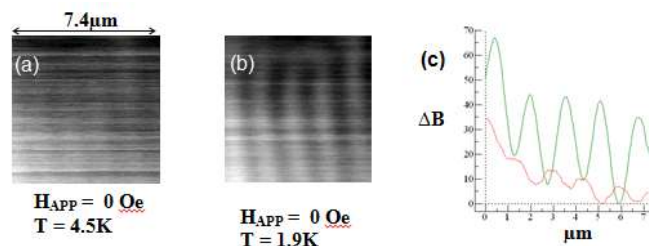


Fig. 8. The temperature dependence of the fine structure. The line scans shown in (c) are an average of the vertical axis. The image size is $\sim 20 \times 20 \mu\text{m}^2$.

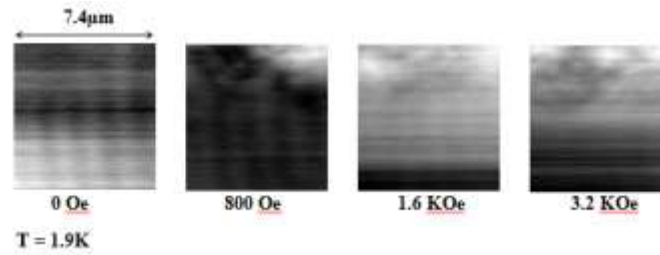


Fig. 9. The Magnetic field dependence of the fine structure. The image size is $\sim 20 \times 20 \mu\text{m}^2$.

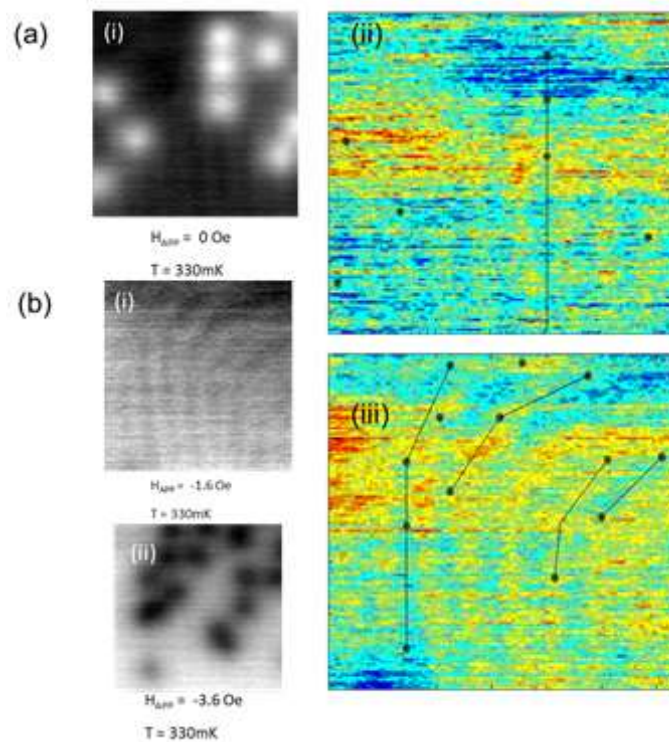


Fig. 10. Some images illustrating attempts to establish an interaction between vortex positions and the underlying magnetic striped structure at two different locations. The image size is $\sim 20 \times 20 \mu\text{m}^2$.

It is clear Scanning tunneling microscope techniques (STM) has best control in scanning Hall probe system which impossible take imaging for chips at the edge of the crystal sample. On the other hand, we find no credible evidence for spontaneous fields that we could attribute to either chiral domain walls or crystal defects anywhere within our samples at very low applied fields. Vortex structures has Very low field which typically highly disordered with highest quality chips (c.f., Fig. 5). Lichtenberg has investigated all experimental data for Sr_2RuO_4 single crystal with a view to creating two sides of bounds (upper and lower) on sizes of area samples with different frames around ($1\mu\text{m}$ to $\approx 50\mu\text{m}$). It has been find minimum detectable fields about ($\sim 0.01\text{G}$) at timescales slower from ($\sim 1\text{s}$) as well as the chiral domain walls at length scales spanning from ($0.8\mu\text{m}$ to $\sim 50\mu\text{m}$) [14]. Through experiments found vortex tubes arrange to a hexagonal lattice in an isotropic s-wave superconductor. But, the Fermi surface with order parameter anisotropies be able to lead to another forms of vortices tubes. Both size and orientation are various of these structures, however, often spacing

with dimensions as well and width of chains/bands which it detected. So, finally observe which it is type I superconducting Ru lamellae are leading to flux exemption and a modulation of the vortex density [15].

4. Conclusions

High resolution of scanning Hall probe microscopy (SHPM) is best magnetic imaging of Sr_2RuO_4 samples. The single crystals Sr_2RuO_4 is not a chiral spin triplet superconductor, which is used scale of spatial resolution about $\sim 0.8\mu\text{m}$. Roots of the differing behavior between samples need to be investigated. Energy considerations of the vortex lattice could provide interesting insights into the exotic physics of this unconventional superconductor. There is no evidence of vortex clustering in our most highly ordered samples at low fields; however the field profiles of isolated vortices do many a unidentified source of broadening. The interaction between vortices seems to dominate over this disorder potential at high temperatures close to critical temperature where pronounced hexagonal vortex ordering is recovered.

References

- [1] Xia, J.; Yoshiteru, M.; Beyersdorf, P. T.; Fejer, M. M. and Kapitulnik, A. (2006). High resolution polar Kerr effect measurements of Sr_2RuO_4 : Evidence for broken time-reversal symmetry in the superconducting state. *Physical Review Letters*, **97** (16):167002.
- [2] Wang, H. et al. (2017). Probing chiral superconductivity in Sr_2RuO_4 underneath the surface by point contact measurements. *New Journal of Physics*, **19**:053001.
- [3] Bending, J. (2012). Vortex Imaging in a Superconductors. *Physica C: Superconductivity*, **479**:65-68.
- [4] Dolocan, V.O.; Lejaya, P.; Mailly, D. and Hasselbach, K. (2006). Observation of two species of vortices in the anisotropic spin-triplet superconductor Sr_2RuO_4 . *Physical Review B*, **74** (14):144505.
- [5] Björnsson, P.G.; Maeno, Y.; Martin and Moler, K. A. (2005). Scanning magnetic imaging of Sr_2RuO_4 . *Physical Review B*, **72** (1):012504.
- [6] Catherine, K. (2012). Chiral p-wave order in Sr_2RuO_4 . *IOP Publishing Ltd*, **75** (4).
- [7] Kallin, C. and Berlinsky, A. J. (2009). Is Sr_2RuO_4 a Chiral P-Wave Superconductor. *Journal of Physics: Condensed Matter*, **21** (16):164210.
- [8] Bending, S.J. (1999). Local magnetic probes of superconductors. *Advances in Physics*, **48** (4):449-535.
- [9] Mao, Z.; Maeno, Y. and Fukazawa, H. (2000). Crystal growth of Sr_2RuO_4 . *Materials Research Bulletin*, **35** (11):1813-1824.
- [10] Kohno, W.; Ueki, H. and Kita, T. (2016). Hall Effect in the Abrikosov Lattice of Type-II Superconductors, *Journal of the Physical Society of Japan*, **85** (8).
- [11] Chen, C.J. (1993). Introduction to scanning tunneling microscopy. 1st ed., Oxford University Press, New York.
- [12] Khomenko, D.; L'vov, V.S.; Pomyalov, A. and Procaccia, I. (2018). Dynamics of the vortex line density in superfluid counterflow turbulence. *Physical Review B*, **97**:014508.
- [13] Marchiori, E., Curran, P.J.; Kim J.; Satchell, N.; Burnell, G. and Bending, S.J. (2017). Reconfigurable superconducting vortex pinning potential for magnetic disks in hybrid structures. *Scientific Reports*, **7**:45182.
- [14] Lichtenberg, F. (2002). The story of Sr_2RuO_4 . *Progress in Solid State Chemistry*, **30**:103-131.
- [15] LIO, Y. and Mao, Z. (2015). Unconventional superconductivity in Sr_2RuO_4 . *Physica C: Superconductivity and its Applications*, **514**:339-353.

ظاهرة الدوامات المغناطيسية فائقة التوصيل ل (Sr_2RuO_4)

حسين علي محمد

قسم الفيزياء ، كلية التربية للعلوم الصرفة ، جامعة كركوك ، كركوك ، العراق

الملخص

تم وصف دراسة الدوامات المغناطيسية الفائقة التوصيل من خلال سلسلة من التجارب المغناطيسية اجريت على الموصلات الفائقة الغير تقليدية التي هي (Sr_2RuO_4) وذلك باستخدام تقنية المجهر النفقي الماسح (SHPM) بدرجة الحرارة الحرجة ($T_C \approx 1.5 \text{ K}$) وفي هذه الدراسة استخدمت العديد من العينات وذلك لتعديل سلوك الدوامات لتقليل كمية الاضطراب فيه. من الناحية التجريبية، أفضل الرقائق المستخدمة تظهر فيه تحولا شفافا للدوامات من مثلث الشكل إلى مربعة الشكل في المجالات المغناطيسية المنخفضة، كما كان متوقعا في حسابات نظرية لندن الموسعة. في تباين صارخ، تظهر شرائح اقل جودة مرتبة بشكل جيد واكثر وضوحه لتسلسل دوامات / النطاقات التي تنسب مبدئيا إلى مصدر خارجي من الاضطراب.